Journal of Materials Chemistry B

Liquid biopsy in combination of solid-state electrochemical sensors and nucleic acid amplification

Journal:	*Journal of Materials Chemistry B*
Manuscript ID	TB-REV-04-2019-000718.R1
Article Type:	Review Article
Date Submitted by the Author:	16-Aug-2019
Complete List of Authors:	Tabata, Miyuki; Tokyo Medical and Dental University, Miyahara, Yuji; Tokyo Medical and Dental University

Journal Name

ARTICLE

Liquid biopsy in combination of solid-state electrochemical sensors and nucleic acid amplification

Miyuki Tabata and Yuji Miyahara *

Received 00th January 20xx,
Accepted 00th January 20xx

DOI: 10.1039/x0xx00000x

www.rsc.org/

Solid-state electrochemical sensors are developing as a new platform for liquid biopsy, combining detection and analysis of nucleic acids with isothermal nucleic acid amplification reactions. For detection of small nucleic acids such as cfDNA, ctDNA and miRNA in liquid biopsy, further development of highly sensitive and precise devices is required to transcend the barrier of classical detection technology. Electrochemical sensors based on engineerng approaches are advantageous for miniaturization of the system and convenience of diagnosis, and the analysis of data obtained with those sensors dovetails with the transition to an information society. This review briefly surveys the current development of electrochemical sensors combined with isothermal amplification for nucleic acid detection and predicts the future direction of research.

1. Introduction

In recent years, liquid biopsy, i.e. diagnosis of body fluids, has come to be recognized among not only healthcare professionals but also patients as a minimally invasive method compared with conventional biopsies involving tissue collection.[1-3] This approach has a great potential clinical significance in screening of diseases, follow-up inspection, and prognosis. The main detection targets of liquid biopsy are cells and nucleic acids circulating in body fluids, which include blood circulating tumor cells (CTCs), cell-free DNA (cfDNA), circulating tumor DNA (ctDNA), exosomes, and micro-RNA (miRNA).

Development of improved clinical platforms for liquid biopsy is urgent in view of its promising potential and marketability, and detection or analysis techniques for the above biomarkers are being developed rapidly through integration of medical/biological knowledge with engineering techniques. In particular, cfDNA and ctDNA are considered to be important biomarkers because they show high correlations with cancer.[4, 5] Because exosomes are contained in urine and saliva, exosomes by themselves or miRNAs in exosomes are drawing attention as promising biomarkers.[6, 7] Exosomes serve as carriers for miRNAs and protect them, enabling miRNAs to circulate in blood without being affected by RNase. Analysis of secreted miRNAs is an active research goal, and over 2600 miRNAs have already been identified by nucleic acid analysis techniques, principally real-time polymerase chain reaction (real-time PCR). Consequently, the correlation between expression levels of specific miRNAs and certain diseases has been revealed. Thus, the development of a new detection platform for cfDNA, ctDNA, and miRNAs is at the forefront of efforts to demonstrate the effectiveness of liquid biopsy not only for disease diagnosis but also prognosis, early diagnosis, preemptive medicine, and healthcare.

For sequence analysis of nucleic acids, next-generation sequencing (NGS) techniques are becoming mainstream. A diversity of tumors and genetic mutations can be analyzed with high sensitivity by the principle of deep sequencing, which carries out multiple sequence analysis using NGS technology. For benchtop-type NGS, miSeq from Illumina Inc., which reads single base extension reactions by fluorescent labeling, and Ion PGM from Thermo Fisher Scientific Inc., which realizes high-precision sequencing based on semiconductor technology, are comparable from the view of performance and cost. The nucleic acid analysis technology based on the existing fluorescent labeling method continues to improve. At the same time, another active research topic is miRNA quantitative detection by devices utilizing biosensing based on electrochemical measurement, which has the advantage of not needing an optical system such as laser excitation light and detector. One example of an electrochemical nucleic acid analysis device useful for liquid biopsy is Ion Torrent (Thermo Fisher Scientific K.K.), which makes use of advanced semiconductor technology. Elsewhere, nanopore devices from Oxford Nanopore Technologies, Inc., which do not require enzymatic elongation reactions or fluorescent labeling, are attracting attention as a more advanced generation of DNA sequencers. Two electrodes are placed across the nanopore, and when a voltage is applied to the system, an ionic current is generated by the electrolyte. By measuring the reduction in ion current as the DNA passes through the nanopore while unwinding the double helix, rapid and precise sequence detection is realized. NGS technologies employing various detection principles have been developed by combining an engineering approach with microfabrication technology.

Electrochemical devices are suitable for microfabrication, making them simple to use and portable.[8-10] Because detection

Institute of Biomaterials and Bioengineering,Tokyo Medical and Dental University, 2-3-10 Kanda-surugadai, Chiyoda, Tokyo 101-0062, JAPAN
Electronic Supplementary Information (ESI) available: [details of any supplementary information available should be included here]. See DOI: 10.1039/x0xx00000x

of circulating nucleic acids related to cancer is made difficult by low sample concentrations, many electrochemical methods in combination with isothermal nucleic acid amplification have been reported.[11, 12] As shown in Fig. 1, the combination of isothermal nucleic acid amplification and electrochemical measurement offers a new analysis method for liquid biopsy. In this review, electrochemical nucleic acid analysis technologies, mainly from 2010 onward, are summarized. Various electrochemical detection approaches, including redox reactions, ion-selective methods, self-assembled monolayer chemistry, and nano-biotechnologies, have been employed to create robust nucleic acid detection platforms. Combined with isothermal amplification methods, these solid-state sensors show great potential as useful devices for liquid biopsy to be employed in precision medicine.

2. Isothermal nucleic acid amplification techniques for electrochemical devices

2.1 Thermal cycling method

The most common nucleic acid amplification method employed by skilled laboratory technicians is the polymerase chain reaction (PCR). The PCR has long been widely used for detection of infectious diseases, food safety, and environmental monitoring. More specifically, real-time PCR is a powerful method for quantitative detection of nucleic acids. In a real-time PCR system, the amplicons are monitored on-the-fly during the PCR reaction, and the time (or the thermal cycle number) required to reach the threshold concentration is highly correlated with the initial copy number of the amplified target nucleic acid. In a real-time PCR instrument, a fluorescent detection system is employed to monitor the amplification process. However, for application of real-time PCR to a miniaturized point-of-care testing device, a fluorescent detection system is relatively bulky and expensive. Therefore, several approaches to miniaturize fluorescent detection have been reported. Electrochemical detection is a potential approach to realize miniaturized and cost-effective detection systems based on real-time PCR.[13, 14] However, the output signals of the electrochemical devices used in combination with real-time PCR are sensitive not only to the production or consumption of the signal molecules during the PCR reaction, but also to the change of electrical properties caused by the programmed thermal cycles. Thus, the detection performance of real-time PCR based on electrochemical devices, in terms of reproducibility and signal-to-noise ratio, is compromised, and the method struggles to achieve a stable measurement. To overcome this problem, various isothermal methods for nucleic acid amplification can be used in combination with electrochemical devices. Typical examples of isothermal amplification methods are rolling circle amplification (RCA),[15-17] helicase-dependent amplification (HDA),[18, 19] nucleic acid sequence-based amplification (NASBA),[20-22] and loop-mediated isothermal amplification (LAMP).[12, 23, 24]

2.2 Linear isothermal amplification

In scenarios requiring small sample volumes and simple detection methods, such as point-of-care testing, linear isothermal amplification methods are preferred to PCR because of the simple procedure and constant operating temperature. Many isothermal amplification methods are available. Among them, RCA is often used in combination with electrochemical detection. Unlike PCR, in which each process of heat denaturation, primer annealing, and extension reaction is strictly controlled by temperature cycling, nonspecific amplification tends to occur easily in the isothermal nucleic acid amplification methods. However, RCA, which employs linear-type amplification, is a particularly popular focus of research because it realizes relatively stable amplification with fewer components. The RCA reaction involves using a strand displacement-type enzyme, specifically a DNA polymerase from the Φ29 bacteriophage, and the extension reaction proceeds at a constant temperature close to room temperature. A short primer DNA or RNA hybridized with a circular probe is extended to a long single-strand DNA or RNA by the Φ29 DNA polymerase. The normal reaction time is approximately 4 hours. In theory, the reaction proceeds until the dNTPs, which are the substrate of the polymerase, are depleted. It is reported that an RCA extended using the circular probe as a mold can concatenate up to 0.5 megabases.[17] Dumbbell probe-mediated RCA (D-RCA) was reported by Zhou et al. for miRNA detection.[25] A dumbbell probe is configured with a miRNA-binding domain (MBD), a SYBR Green dye-binding domain (SGBD), and a loop domain. After binding of target miRNA and MBD, the RCA reaction occurs in the presence of T4 DNA ligase and Φ29 polymerase. This method achieves a wide detection range (1 fM–100 nM) of miRNA, and the background signals of negative controls are significantly lower than those observed in the target samples. D-RCA has been reported to provide a highly sensitive approach for clinical diagnostics.

In summary, detection of nucleic acids based on RCA is clinically useful. Although RCA-based plasmid preparation kits are commercially available, their application to diagnostic instruments in liquid biopsy is still at the research stage.

2.3 Exponential isothermal amplification

In linear amplification methods such as RCA, the number of nucleic acid molecules does not change before and after the reaction, and the molecules that can be targets for sensing, such as byproducts released in the amplification process, also increase only linearly. Therefore, several modified RCA methods have been reported, which realize an increase in reaction speed by incorporating an exponential amplification mechanism.[26, 27] Such modified RCA reactions are advantageous for electrochemical signal amplification, and devices for electrochemical nucleic acid quantification utilizing the modified RCA reactions have attracted attention. Here, some modified RCAs that exponentially amplify the targets are described. Hyper-branched RCA[15, 28] is performed by an extension reaction of forward primers that bind to circular probes (detection targets). After the reverse primers bind to the elongated forward primers, copious extension processes

proceed at the downstream DNAs. Primer-generation RCA (PG-RCA), developed by Murakami et al.,[29] achieves multiple primer generation during the reaction by incorporating a nicking site in the circular probe, resulting in exponential amplification. In addition, Murakami et al. proposed a method for detecting RNA that suppresses nonspecific amplification by forming a three-way junction (3WJ).[30] The 3WJ formation was combined with PG-RCA reaction (Fig. 2a). Specifically, 3WJ probes (primer and template) hybridize to the target RNA to form a 3WJ structure, and then DNA primers (signal primers) are generated from the 3WJ structure extension. The signal primer cleaved by the nicking reaction binds to the circular probe and the following round of PG-RCA is initiated. In this 3WJ method, because the RCA reaction is performed by displacing the non-template strand, the sequence of reactions of the circular probe is repeated.

LAMP, another widely used isothermal nucleic acid amplification method, is more robust than PCR, and is very well established in the fields of bacterial and viral assay (Fig. 2b).[23] Many types of detection kits for *in-vitro* diagnosis and environmental science are commercially available from Eiken Chemical Co., Ltd., the original developer of the LAMP reaction. The principle of the LAMP reaction is to perform strand displacement with Bst DNA polymerase at a constant temperature, like in many isothermal amplification reactions. By mixing target DNA, primers (i.e. FIP, F3 Primer, BIP, and B3 Primer), Bst DNA polymerase, and dNTP in the appropriate LAMP buffer, the LAMP reaction occurs at a constant temperature around 65 °C after hybridization of four primers to six regions of the target DNA. The DNA amplification efficiency is high enough to increase the signal by a factor of 10^9 to 10^{10} in 15 minutes to 1 hour. When reverse transcriptase is added to the LAMP mixture, RNA can be amplified in one step as in the case of DNA. LAMP is already established as a reliable amplification system; however, some remaining problems, such as the expensive reagents (a consequence of the use of at least four primers) and the need for careful design of the primer sets, may be a stumbling block to its wider application.

3. Solid-state electrochemical sensors detecting nucleic acids

Various types of electrochemical sensors have been developed to realize simple, rapid, sensitive, and inexpensive multiplexed analysis of nucleic acids for point-of-care-testing and liquid biopsy. Several kinds of simple electrodes are capable of signal transduction from a molecular recognition signal or amplified nucleic acid signal to an electrical signal in an electrochemical detection system. This method is, therefore, suitable for miniaturization of the complete detection system, mass-production of the sensors, and integration of the sensors for parallel multi-analyte detection, in contrast to other analytical systems. Gold, platinum, graphite, glassy carbon, and silver/silver chloride are the most often used electrode materials, sometimes in combination with various kinds of nanoparticles, nanotubes, or graphene. The electrochemical or electrical signals are generated directly via the properties of the nucleic acid or with the use of electroactive reporter molecules, which induce changes in current, potential, or impedance at the electrodes.

In the next sections, we will focus on the different types of electrochemical sensors used for nucleic acid detection in combination with isothermal amplification, including chronocoulometry[31], ion-selective electrodes[32-35], amperometry[36-39], and field-effect transistors[14, 34-39], while voltammetry is frequently used in combination with isothermal amplification as listed in Table 1.

3.1 Chronocoulometry

Detection of redox reactions on electrodes is one of the most common electrochemical methods for detecting nucleic acids.[40-42] As shown in Fig. 3. Yao et al. performed solid-phase RCA on the surface of a Au electrode to quantitatively detect miRNA.[31] The RCA products were detected *in situ* using chronocoulometry (CC) with ruthenium (III) hexaammine (RuHex) as the signaling molecule. CC is a charge detection method in which an electric potential is applied stepwise in two steps. The obtained current is integrated as a function of time, and converted into a charge amount. When an electrically active chemical species such as a redox marker is consumed in response to the electrode reaction, the obtained current value depends on the speed at which the electroactive material diffuses near the working electrode. The amount of current follows the Cottrell equation. Specifically, the charge Q, which is a function of time, is expressed by the expanded Cottrell equation (Eq. 1).

$$Q = 2FnAC_b\left(Dt/\pi\right)^{1/2} + Q_c + Q_{ads} \quad \text{Eq. 1}$$

where F is the Faraday constant, n the number of electrons involved in the electrode reaction, A the electrode area (cm^2), C_b the bulk concentration (mol cm^{-3}), D the diffusion coefficient ($cm^2\ s^{-1}$), t the time (s), Q_c the capacitive charge (coulomb), and Q_{ads} the charge produced by the adsorbed reactant. From Faraday's law, Q_{ads} can be expressed by Eq. 2.

$$Q_{ads} = nFA\Gamma \quad \text{Eq. 2}$$

where Γ is the quantity of adsorbed reactant (mol cm^{-2}). As a cationic redox marker, RuHex can be electrostatically trapped onto every three of phosphate groups of nucleic acids. CC is able to give a direct signal proportional to the number of phosphate groups of nucleic acids at the electrode surface in the presence of cationic redox markers. In CC measurement, a gold sensor chip is used to integrate the working electrode, reference electrode, and counter electrode. Thiolated DNA probe 1, having a partially complementary sequence to that of microRNA143 (miR-143), is immobilized on the working electrode via chemical bonding between thiolate and gold. The amount of immobilized DNA probe 1 determined by CC is from 1×10^{12} to 6×10^{12} molecules per cm^2. After hybridization of DNA probe 2, which has a partially complementary sequence with both DNA probe 1 and the target miR-143 on the electrode surface, solid-phase RCA was performed for a fixed time at 30 °C. The solid-phase RCA reaction was found to reach equilibrium in 2 hours and the detection sensitivity of RCA-CC assay was 100

fM. To apply this RCA-CC system for liquid biopsy, miR-143 was spiked into human blood and extracted as total RNA, and then RCA-CC assay was performed. The detection range was 1 pM–1 nM and the detection sensitivity was 1 pM. Thus, quantitative detection of miRNA was accomplished by RCA-CC assay. However, some aspects remain to be improved, such as the fact that this assay requires 2 hours of reaction time and is an endpoint assay.

3.2 Ion-selective electrodes

In a nucleic acid extension reaction catalyzed by a polymerase, when one dNTP is bound to the template strand, one pyrophosphate and one proton are released as by-products. Pyrosequencers or proton sequencers that detect these ions are already commercially available. One of the most successful examples of commercialized products is the Ion Torrent (Thermo Fisher Scientific) semiconductor chip-based DNA sequencer launched in 2012.[13, 14] As shown in Fig. 4, millions of ion-sensitive field-effect transistors (ISFETs), which detect protons released during single-base extension reaction, are integrated into the chip, which acts as a well. Using these ion detection principles, ion-selective electrodes have been developed for liquid biopsy application.[32] Needle-type iridium/iridium oxide (Ir/IrO_x), which is a typical proton-sensitive material, was employed for electrochemical monitoring of PG-RCA in a real-time and label-free manner. The target DNA was detected in the range of 10 pM–1 nM. Sanjoh et al. succeeded in electrochemical detection of pyrophosphate by synthesizing a boronic acid derivative that specifically interacts with pyrophosphate and immobilizes it on an electrode.[43] Further pyrophosphate experiments combined with signal amplification reactions are awaited.

As mentioned in section 2.2 and 2.3, the linear RCA reaction often performs poorly in combination with electrochemical detection of nucleic acids. To accelerate the isothermal amplification reaction, Seich et al. focused on PG-RCA and performed real-time monitoring of DNA amplification in the presence of ethidium bromide (EtBr) using an ethidium ion (Et^+)-selective microelectrode.[33] In detail, a PG-RCA mixture containing a cyclic probe, dNTP, Φ29 DNA polymerase, Nb.BbvCI nicking endonuclease, EtBr, and target DNA (1 μM, 100 nM, 10 nM) was prepared in advance according to the reported method by Murakami et al. The potential change was monitored as the PG-RCA extension reaction was performed at 37 °C for 2 hours. As the PG-RCA progressed, the Et^+ concentration in the system decreased due to intercalation. As a result, the potential monitored by the Et^+-sensitive microelectrode decreased as the extension reaction proceeded. Because the electrical properties of the Et^+ microsensor follow the Nernst equation expressed by Eq. 3, PG-RCA can be detected electrochemically in real time.

$$E = E_0 + \left(2.303^{RT}/_{zF}\right)\log a \quad \ldots \text{ Eq. 3}$$

where E_0 is the standard electrode potential, R the ideal gas constant, T the temperature in Kelvin, z the number of moles of electrons, F the Faraday constant, a the ion activity. As mentioned earlier, the potential change during PG-RCA progression decreases as the elongation reaction proceeds, as the free Et^+ concentration in the PG-RCA mixture decreases. In Ref. 37, when the target DNA concentration was 1 μM, the reaction finished in approximately 40 min, and the potential decreased by about 60 mV. This result is equivalent to about 90% consumption of free Et^+ in the PG-RCA solution. Thus, quantitative detection of amplified nucleic acid with an Et^+ microsensor was demonstrated. However, the construction of a detection system that does not require a labeling agent such as SYBR Green has been a challenge.

3.3 Amperometry

Biomolecule immobilization technology on precious metal surfaces such as gold, silver, and platinum using self-assembled monolayer (SAM) formation by thiol and disulfide derivatives is widely used for its simplicity of operation. In the case of gold, the orientation process for the covalent bonding of Au-S has been studied in detail,[42, 44-46] and SAM formation techniques for thiolated peptides and thiolated DNA are applied in electrochemical devices, the quartz crystal microbalance (QCM), and surface plasmon resonance (SPR). To enhance the sensitivity of the biosensor and improve the signal-to-noise ratio, functional groups such as polyethylene glycol (PEG) chains or sulfobetaine groups can be introduced via Au-S bonding to suppress nonspecific adsorption.

SAMs immobilized on gold nanoparticles (AuNPs) are often used as a foothold for initiating isothermal amplification. The determination of *Leishmania* DNA through the use of isothermal recombinase polymerase amplification (RPA) was reported.[47] The primers were labelled with methylene blue and AuNPs and detected with chronoamperometry, resulting in detection of parasite concentrations in the logarithmic range of 0.5–500 parasites mL^{-1} of blood.

When the probe molecule is a nucleic acid aptamer that captures the target protein, electrochemical signal amplification is accomplished by isothermal amplification of the probe molecule itself. To screen aptamers capable of detecting neutrophil gelatinase-associated lipocalin (NGAL), electrochemical sandwich assays on Au-electrode-modified DNA–*p*-aminothiophenol SAMs were performed.[36] The experiments showed a moderate capture ability of one of the aptamers (LCN2–4). Subsequently, RCA was employed in combination with this aptamer to improve electrochemical detection. NGAL molecules covalently linked to magnetic beads (MBs) were employed for aptamer recognition on the MBs, and RCA was performed with the addition of a padlock probe, T4 DNA ligase, dNTP, and Φ29 polymerase. The functional affinity of this aptamer was enhanced by three orders of magnitude using RCA, and the reaction was completed in only 15 min.

Moura-Melo et al. reported the helicase dependent isothermal amplification (HDA) in combination with chronoamperometric detection using a gold electrode with SAM modification to detect a transgene from the Cauliflower Mosaic Virus 35S Promoter (CaMV35S), which was inserted into most transgenic plants. In this method, the end point detection was performed after isothermal amplification for 40-60 min

instead of real-time monitoring during nucleic acid amplification. Although nonspecific amplification took place to some extent, the byproducts were not detected and Yes/No detection of genetically modified organisms (GMOs) was achieved with a limit of detection of ~30 copies of the CaMV35S genomic DNA. The development of sensitive, rapid, robust, and reliable methods for the detection of GMOs is crucial for proper food labeling[48].

The LAMP reaction was designed in a liquid flow channel and real-time monitoring of the amplified products was performed using a gold electrode and ruthenium hexaamine (RuHex) as a redox indicator. The primers for the LAMP reaction were immobilized on the liquid-flow channel at five different positions, with an interval of approximately 10 mm between positions. The primers were adsorbed and dried on the edge of the flow channel. A LAMP solution containing a sample nucleic acid, *Tin* DNA polymerase, and RuHex was introduced to the flow channel to initiate the LAMP reaction. Linear sweep voltammetry was performed to detect redox current based on RuHex. This system was applied to detect mature miRNA extracted from serum, which was extended to about 100 base pairs by reverse-transcription and elongation reactions in advance. The initial number of miRNA copies was correlated with the time when the cathodic current began to increase. Five miRNAs were simultaneously detected at 103−106 copies per 50 μL within 2 h[49].

Sensitive method for miRNA detection was designed using carbon nanotube (CNT) with hairpin probe triggered solid-phase RCA. In the presence of miRNA, the stem-loop structure was unfolded, triggering the RCA process. Due to the efficient blocking effect originating from the polymeric RCA products, the label-free assay of miRNA exhibits an ultrasensitive detection limit of 1.2 fM. The protocol possesses excellent specificity for resolving lung cancer-related let-7 family members which have only one-nucleotide variations[50].

Silver nanoclusters (AgNCs) were synthesized on the electrode surface after hybridization chain reaction (HCR) amplification to form dsDNA polymers with numerous C-rich loop DNA templates on the electrode surface. The target miRNA-199a hybridizes with the partial dsDNA probes to initiate the target assisted polymerization nicking reaction to produce massive intermediate sequences, which can be captured on the sensing electrode by the self-assembled DNA secondary probes. DNA-templated synthesis of AgNCs could be realized by subsequent incubation of the dsDNA polymer-modified electrode with $AgNO_3$ and sodium borohydride. The amount of in situ synthesized AgNCs dramatically increased, leading to substantially enhanced current response for highly sensitive detection of miRNA. With this method, the lower detection limit of miRNA-199a was 0.64 fM[51].

3.4 Field-effect transistors

Since the first successful use of field-effect transistor (FET) devices to detect single base extension reactions in DNA sequencing,[13, 52] they have also been applied to monitor nucleic acid amplification for quantitative detection of nucleic acids.

Toumazou et al. developed an integrated chip for real-time monitoring of pH changes during nucleic acid amplification using an ISFET, exploiting the fact that protons are released during the nucleotide incorporation process in nucleic acid amplification (Fig. 5). The amount of hydrogen ions released is dependent on the initial concentration of target nucleic acid, and quantitative analysis of nucleic acid can be realized in a label-free and non-optical way. Signal processing circuits, temperature sensors, and heaters were integrated with ISFETs in a chip. The ISFET chips were combined with PCR or LAMP methods for genotyping the cytochrome P450 family from crude human saliva, and discrimination of unique single-nucleotide polymorphism (SNP) variants was achieved (Fig. 6).[14]

Gao et al. used a silicon nanowire (SiNW) transistor in combination with RCA for sensitive and specific detection of hepatitis B virus (HBV) DNA (Fig. 7). The signal of the SiNW transistor was significantly amplified by the binding of an abundance of repeated sequences of RCA products. HBV DNA at a concentration of 1 fM could be detected with a signal-to-noise ratio of more than 20 in a direct and label-free manner. SNP discrimination was achieved, which indicated the high specificity of this method.[37]

A thin-film transistor (TFT) based on nanoribbons has been developed for rapid real-time detection of pH change during DNA amplification using an isothermal RPA method. This method was applied to detect two genes, CTX-M and NDM, which are involved in conferring bacterial resistance against antibiotic agents of the cephalosporin and carbapenem class, respectively. In the treatment of infectious disease, antimicrobial resistance is rapidly becoming a global threat. It is important to develop rapid and sensitive tests to determine antibiotic resistance for diagnosis and treatment of infectious disease. Using the TFT-based system combined with RPA, it was shown that up to 10 copies of the gene in genomic DNA extracted from *E. coli* or *K. pneumoniae* clinical isolates could be detected within a few minutes (Fig. 8).[34]

Carbon materials, especially carbon nanotubes and graphene, have been actively studied as electrochemical sensor materials because of their excellent electrical properties. The carrier mobility in graphene on silicon substrates is reported to be 10,000 $cm^2/V{\cdot}s$, rising to 200,000 $cm^2/V{\cdot}s$ in the crosslinked state. These values are greater than those of silicon (1,500 $cm^2/V{\cdot}s$) and organic transistors (generally less than 10 $cm^2/V{\cdot}s$). Because pristine single-walled carbon nanotubes and graphene do not have functional groups, oxidation treatment is used to introduce hydroxyl or carboxyl groups and immobilize ligand molecules by covalent bonding. In addition, ligand molecules are introduced by π-π stacking, an intermolecular interaction, using characteristic structures containing C-C bonds. In search of two-dimensional materials beyond graphene, research into other transition metal dichalcogenides (TMDCs) such as hexagonal boron nitride (h-BN) and molybdenum disulfide (MoS_2) has also been expanding rapidly worldwide. Graphene was used to fabricate a solution-gated FET structure with on-chip co-planar electrodes, and a polydimethylsiloxane-based microfluidic reservoir. A linear pH response with a slope of about 0.23 V/pH was obtained using buffers in the pH range 5–

9. By combining the graphene FET with microscale LAMP, the amplification process of a lambda phage gene was monitored in a real-time manner. During amplification, protons were released, which gradually altered the Dirac point voltage (V_{Dirac}) of the graphene FET. The resulting detection limit of the graphene FET was at the femto-molar level. An amplification of 10 ng/μL DNA for 1 h generated a change of the Dirac point voltage, ΔV_{Dirac}, of 0.27 V. The device showed a limit-of-detection of 2×10^2 copies/μL of viral DNA (Fig. 9).[35]

Elsewhere, sensing electrodes for an extended gate FET were fabricated on flexible and transparent polyethylene naphthalate substrates. A thin film of tantalum oxide was sputtered on the sensing electrode to form a pH sensor. The extended gate was connected to a commercial MOSFET for signal transduction from pH values to electrical signals. The flexible thin-film sensor was combined with real-time isothermal nucleic acid amplification methods such as LAMP and RCA techniques for label free gene expression profiling of two cancer biomarker genes, c-MYC and BCR-ABL1. In the case of the LAMP reaction, a linear relationship between the log copy number of the initial template c-MYC DNA (10^8 to 10^{11} copies) and the threshold time was obtained. The developed system was also used in combination with RCA for direct quantification of RNA targets at room temperature, which led to elimination of external temperature controllers and simplification of the diagnostic procedures (Fig. 10).[38]

A dual-gate ISFET array platform with 1024 × 1024 sensors was developed and combined with on-chip LAMP reactions for electrical detection of foodborne bacterial pathogens. The size of the dual-gate ISFET array chip was 7 × 7 mm^2 and multiple chambers with a volume of 250 nL were fabricated on each chip. The pH changes triggered by the amplification reaction in each chamber could be monitored independently with 3500 FETs. To maximize the signal-to-noise ratio and improve the reliability of the results, the output of the high-density FET array was treated with a group of data analysis techniques such as redundancy techniques. Using the developed platform, the on-chip electrical detection and identification of the targeted eae and invA genes for *E. coli* O157 and *S. typhi*, respectively, was achieved with parallel LAMP assays. The LAMP reactions were specific, without false positives, and the lower detection limit was 23 CFU per reaction on the chip.[39]

4. Application to real-world samples

Electrochemical detection methods in combination with isothermal nucleic acid amplification or signal amplification have been applied to real-world samples. Several examples of the above approaches to evaluate real samples are listed in Table 1. Target nucleic acids are mainly categorized into microRNAs, clinically relevant nucleic acids, and nucleic acids of bacteria or viruses. The starting samples and the sample preparation methods are dependent on the target nucleic acid to be detected.

Table 1 Examples of real sample applications.

Target	Electrochemical methods	Amplification methods	Samples	Results	Ref.
microRNA-21	Differential pulse voltammetry (DPV)	Locked nucleic acid strand displacement reaction	Exsomal microRNA from breast cancer cell line MCF-7 or non-cancer cell line CHO-K1	The results are in good agreement with the findings of the PCR method. Limit of detection: 67 aM	53
microRNA-196a	Square wave voltammetry (SWV)	Enzymatic signal amplification and template-free DNA extension reaction	MicroRNA-196a spiked in 100-fold-diluted plasma	Recovery values ranged from 97.6% to 102.2%. Limit of detection: 15 aM	54
microRNA-21 microRNA-141	Differential pulse voltammetry (DPV)	target-triggered hybridization chain reaction (HCR)	lysate of MCF-7 cells	The concentrations of miR-141 and 21 are 2.55 fM and 1.97 pM, demonstrating overexpression of miR-21 in MCF-7 cells. Limit of detection: 280 aM and 360 aM for miR141 and miR21	55
microRNA-21	Differential pulse voltammetry (DPV)	miRNAs-initiated cleavage of DNA by duplex-specific nuclease	five human serum samples of breast cancer patients	The results are in good agreement with those of qRT-PCR, confirming the practical performance. Limit of detection: 86 aM	56
microRNA-21	Differential pulse voltammetry (DPV)	phi29-mediated isothermal strand-displacement polymerase reaction	RNA extracted from human breast cancer tissues and paired adjacent tissues	The results were consistent with the RT-PCR results. Limit of detection: 9 fM	57

microRNA-21	Differential pulse voltammetry (DPV)	T4 RNA ligase 2 and T7 exonuclease to catalyze the cyclic enzymatic reaction	miRNA-21 in blood serum of gastric cancer patients.	The results are in good accordance with the qTR-PCR. Limit of detection: 360 aM	58
microRNA-21	Amperometry with screen-printed carbon electrodes	Hybridization chain reaction (HCR) amplification	RNA was extracted from a breast-cancer cell line (MCF-7) and non-tumorigenic cells.	miR-21 over-expression levels in tumor tissues were in good agreement with the reported range. Limit of detection: 60 pM	59
microRNA-21	Differential pulse voltammetry (DPV)	Arched probe mediated isothermal amplification reaction	miR-21 was extracted from MCF-7 cells. The diluted RNA sample were spiked with synthetic miR-21.	A recovery ratio was 93.3%. Limit of detection: 50 aM	37
maternally expressed gene3 (MEG3) lnRNA	Differential pulse voltammetry (DPV)	Coupling RNase A-aided target recycling	Serum samples from the Hospital. The target strands mixture was spiked into diluted serum.	The recovery results were 95.2–104.3% for T1 and 94.6–104.6% for T2. Limit of detection: 250 aM for T1 and 300 aM for T2	60
c-MYC and BCR-ABL1 genes	Potentiometry with ISFET	Loop-mediated isothermal amplification (LAMP) Rolling Circle Amplification (RCA)	K562 (BCR-ABL1 positive cell line) was derived from a chronic myeloid leukemia (CML) patient.	Clear discrimination of DNA concentration, comparable to that of standard technologies. Limit of detection: 10^8 copies	38
CTX-M and NDM genes	Potentiometry thin-film transistor (TFT)	Isothermal recombinase polymerase amplification (RPA)	Strains expressing the target resistance genes were isolated from human clinical sample.	The assay performed on the TFT sensor is faster than that of the fluorescent assay. Limit of detection: 10^4 copies	34
Human papilloma viruses (HPVs)	Chronocoulometry (CC) Cyclic voltammetry (CV)	Endonuclease-assisted strand displacement amplification (SDA)	Cervical carcinoma Hela cell line as HPV positive and Lovo cell lines as HPV negative were used.	The signal was negligible for the Lovo cell line and the increase was recorded for the Hela cell line. Limit of detection: 0.1 pM	61
Hepatitis C virus (HCV)	Squarewave anodic stripping voltammetry (SWASV)	Isothermal circular strand-displacement polymerization (ICSDP) reaction	5 clinical serum specimens containing HCV RNA (Henan Provincial Peoples Hospital).	The results assayed were comparable with those obtained by the automated PCR amplification. Limit of detection: 2.3 pM	62
Vibrio cholerae serogroups O1 and O139	Amperometry with the presence of electroactive α-naphthol	Dry-reagent-based nucleic acid amplification assay	Bacterial strains consisting of 95 positive samples and 73 negative samples.	Excellent diagnostic sensitivity and specificity (100%) for 168 spiked stool samples. Limit of detection:10CFU/ml for both V. cholerae O1 and O139	63
Mycobacterium tuberculosis (MTB)	Square wave voltammetry (SWV)	Loop-mediated isothermal amplification (LAMP)	The bacterial culture samples of MTB, HIN, and KPN from clinical sputum specimens were used.	The quantitative detection using μME-LAMP system with lysed bacteria of MTB Limit of detection: 28 copies/ μL for MTB	64

In the detection of microRNAs, the starting samples are exosomes, cancer cell lines, tissues, serum, and plasma from cancer patients, from which microRNAs are extracted. The extracted RNA or serum samples are sometimes spiked with standard solutions containing synthetic micro RNA. These samples are used to evaluate the matrix effect of the real-world samples and the recovery rate of the proposed detection methods. For example, Ma et al. used magnetic micro-carriers with immobilized oligonucleotides to assist the isothermal strand-displacement polymerase reaction and measured the anodic current of the screen-printed carbon electrode for quantitative detection of microRNA-21.[57] The target microRNA-21 was located in the RNA extracted from human breast cancer tissues and paired adjacent tissues. Five breast carcinoma tissues and the same paracancerous tissues were obtained from the breast oncology center of a university hospital. All breast tumors were confirmed by surgery and pathology. Total RNA was extracted with a commercial miRNA isolation kit. The electrochemical signal intensities from the breast cancer tissues were clearly higher than those from the adjacent control tissues.

In addition, the results were consistent with those of reverse transcription PCR (RT-PCR).

In the detection of nucleic acids of bacteria or viruses, bacterial culture samples or human serum are used as real-world samples. Lu et al. developed an electrical monitoring platform for sensitive detection of hepatitis C virus (HCV) using cytosine–Ag^{+}–cytosine coordination chemistry in combination with an isothermal circular strand-displacement polymerization reaction.[62] Silver ions captured on the screen-printed carbon electrode during the reaction were detected with square wave anodic stripping voltammetry. Five clinical serum specimens containing HCV RNA were obtained from the clinical laboratory of a hospital. The assayed data were compared between the proposed method and a commercialized Cobass Amplicor HCV Test Analyzer, which is based on automated PCR amplification and fluorescent detection of HCV RNA. The relative standard deviation values between the two methods were lower than 8.7% and good correlation was obtained between the two methods.

In summary, electrochemical detection methods in combination with isothermal nucleic acid amplification or signal amplification have been increasingly used to evaluate real-world samples and demonstrated to have a comparable assay performance to the conventional methods.

5. Future perspectives

During the last 10 years, liquid biopsy research for cancer has been dramatically progressed. Materials derived from tumors include circulating tumor cells (CTCs), circulating tumor DNA (ctDNA), microRNA, protein markers and extracellular vesicles such as exosomes. Cell-free DNA (cfDNA) present in the blood plasma or other bodily fluids (urine, ascites) can be categorized in terms of base length. There are the smaller size fragments (approximately 150 bp) that originate from apoptotic fragmentation of genomic DNA inside a cell. DNA fragments of apoptotic origin are also present in healthy people. On the other hand, there are the larger size fragments that originate mainly from necrotic cell death (necrosis). When a tumor cell dies, it releases DNA molecules into the blood stream as ctDNA.

Some studies revealed that significantly higher concentrations of cfDNA were found in cancer patients and that simple quantification of cfDNA can confirm the presence of cancer or disease-free status and relapse after curative surgery[65, 66]. Other studies demonstrate that solely the amount of cfDNA is not a useful diagnostic tool and that the utility of cfDNA is limited without knowledge of tumor mutations[67, 68]. Recently, several studies have shown that key cancer mutations can be detected in liquid biopsies, reflecting those detected in traditional tumor biopsies[69-73]. Tumor genotyping is one possible method of categorizing tumors for clinical decisions and has the potential to identify patients who will likely respond to various drugs. A consensus on reliable and efficient methods for cfDNA quantification and analysis is essential for the clinical evaluation of ctDNA as a liquid biopsy to obtain more consistent data that can be compared in different laboratories.

One of the most important biological issues is intratumoral heterogeneity. Almost all tumors treated with any therapy acquire resistance as a result of tumor heterogeneity, clonal evolution, and selection. Since therapy-related markers may change throughout tumor progression, biomarker detections at multiple time points will provide crucial information for patient management. To overcome these issues, methods and technologies will be needed for a rapid, cost-effective, and noninvasive identification of biomarkers at various time points during the course of disease, while real time PCR, next generation sequencing, and array-based methods are used to detect cfDNA, ctDNA and microRNA in plasma and serum.

According to several studies of liquid biopsy approaches in cancer patients, the success rate of liquid biopsy is related to the tumor mass as well as the tumor stage of a patient at the time of liquid biopsy. The liquid biopsy has been shown to be minimally successful, when tumor mass is low, due to the limited number of tumor cells dying and thereby releasing DNA into the blood. The success rate of liquid biopsy is tumor type, stage, and mass dependent. Another issue to make the liquid biopsy difficult is the contamination of tumor cell-derived DNA, with DNA coming from unrelated processes naturally occurring in the body.

Sensitivity of the liquid biopsy may be superior for detecting cancer at a very early stage, such as in cases of reoccurrence of cancer after curative surgery, or in a population-based screening program. The potential of the liquid biopsy in the field of clinical cancer research is being clearly recognized and a liquid biopsy is now frequently embedded in the design of several clinical trials. However, for actual implementation of the liquid biopsy in clinical practice, it is necessary to develop standardized pre-analytical and analytical methodologies, including blood collection, processing, and storage and DNA extraction, quantification, and validation in large prospective clinical studies. Once the limitations within this field are overcome, there is great potential for new technologies to have a profound impact on early-stage diagnosis within oncology, which would contribute to higher survival rates.

In the future information society, a huge amount of information from sensors in the physical world will be accumulated in cyberspace. This big data will be analyzed by artificial intelligence (AI) and fed back in various forms to the real human society. The automated analysis of an enormous amount of big data, beyond the abilities of human beings, is expected to deliver previously unrealizable benefits to industry and society. The sensors described in this review will be the input part of this information system and are key technologies to produce big data based on high-quality information. In the field of medical treatment and diagnosis, technologies to acquire biometric information non-invasively and without constraints have been developed. However, our ability to obtain biological and medical information by external physiological monitoring, in order to realize preemptive medicine, early diagnosis, and healthcare, is currently limited. Through liquid biopsy, it is possible to collect samples in non-invasive and minimally invasive ways, using body fluids such as urine and saliva as samples in addition to blood.[8, 10, 74]

Furthermore, because extracellular nucleic acids and extracellular vesicles contained in body fluids carry information on parent cells in the body, it is expected that more accurate biological and medical information can be obtained. In liquid biopsy, therefore, cells and nucleic acids circulating in body fluids are detection targets, and various diagnostic methods and their platforms have been actively investigated.

6. Conclusions

The capacity to achieve rapid, sensitive, specific, quantitative, and multiplexed genetic detection of diseases via a robust, portable, point-of-care platform could transform many diagnostic applications. While contemporary technologies have yet to effectively achieve this goal, the advent of microfluidics provides a potentially viable approach to this end by enabling the integration of sophisticated multistep biochemical assays (e.g., sample preparation, genetic amplification, and quantitative detection) in an all-in-one, portable device from relatively small biological samples.

Integrated electrochemical sensors with isothermal amplification methods offer a particularly promising solution to genetic detection because they do not require optical instrumentation and are readily compatible with both integrated circuits and microfluidic technologies. Nevertheless, the development of generalizable microfluidic electrochemical platforms that integrate sample preparation and amplification as well as quantitative and multiplexed detection remains a challenging and unsolved technical problem. Recognizing this unmet need, a series of microfluidic electrochemical DNA sensors that have progressively evolved to encompass each of these critical functionalities have been developed.

Conflicts of interest

There are no conflicts to declare.

Acknowledgements

This work was supported in part by the Center of Innovation Program from Japan Science and Technology Agency, JST, the Ministry of Education, Culture, Sports, Science and Technology (MEXT) as part of the Research Center for Biomedical Engineering, JSPS KAKENHI Grant-in-Aid for Young Scientists (B) (No. 15K16320), and JSPS KAKENHI (No. 18K18361).

References

1. E. Crowley, F. Di Nicolantonio, F. Loupakis and A. Bardelli, *Nat. Rev. Clin. Oncol.*, 2013, **10**, 472-484.
2. C. Alix-Panabieres and K. Pantel, *Clin.l Chem.*, 2013, **59**, 110-118.
3. C. Alix-Panabieres and K. Pantel, *Canc. Disc.*, 2016, **6**, 479-491.
4. E. Vilar and J. Tabernero, *Nature*, 2012, **486**, 482-483.
5. L. A. Diaz, R. T. Williams, J. Wu, I. Kinde, J. R. Hecht, J. Berlin, B. Allen, I. Bozic, J. G. Reiter, M. A. Nowak, K. W. Kinzler, K. S. Oliner and B. Vogelstein, *Nature*, 2012, **486**, 537-540.
6. Y. Yoshioka, N. Kosaka, Y. Konishi, H. Ohta, H. Okamoto, H. Sonoda, R. Nonaka, H. Yamamoto, H. Ishii, M. Mori, K. Furuta, T. Nakajima, H. Hayashi, H. Sugisaki, H. Higashimoto, T. Kato, F. Takeshita and T. Ochiya, *Nat. Commun.*, 2014, **5**.
7. H. Im, H. L. Shao, Y. I. Park, V. M. Peterson, C. M. Castro, R. Weissleder and H. Lee, *Nat. Biotechnol.*, 2014, **32**, 490-U219.
8. M. Hasanzadeh, N. Shadjou and M. de la Guardia, *Trac-Trend. Anal. Chem.*, 2017, **91**, 67-76.
9. Q. Liu, S. Y. Lim, R. A. Soo, M. K. Park and Y. Shin, *Biosens. Bioelectron.*, 2015, **74**, 865-871.
10. N. Bellassai and G. Spoto, *Anal. Bioanal. Chem.*, 2016, **408**, 7255-7264.
11. S. Campuzano, P. Yanez-Sedeno and J. M. Pingarron, *Sensors*, 2017, **17**.
12. K. W. Hsieh, A. S. Patterson, B. S. Ferguson, K. W. Plaxco and H. T. Soh, *Angew. Chem. Int. Edit.*, 2012, **51**, 4896-4900.
13. J. Rothberg, W. Hinz, T. Rearick, J. Schultz, W. Mileski, M. Davey, J. Leamon, K. Johnson, M. Milgrew, M. Edwards, J. Hoon, J. Simons, D. Marran, J. Myers, J. Davidson, A. Branting, J. Nobile, B. Puc, D. Light, T. Clark, M. Huber, J. Branciforte, I. Stoner, S. Cawley, M. Lyons, Y. Fu, N. Homer, M. Sedova, X. Miao, B. Reed, J. Sabina, E. Feierstein, M. Schorn, M. Alanjary, E. Dimalanta, D. Dressman, R. Kasinskas, T. Sokolsky, J. Fidanza, E. Namsaraev, K. McKernan, A. Williams, G. Roth and J. Bustillo, *Nature*, 2011, **475**, 348-352.
14. C. Toumazou, L. M. Shepherd, S. C. Reed, G. I. Chen, A. Patel, D. M. Garner, C. J. A. Wang, C. P. Ou, K. Amin-Desai, P. Athanasiou, H. Bai, I. M. Q. Brizido, B. Caldwell, D. Coomber-Alford, P. Georgiou, K. S. Jordan, J. C. Joyce, M. La Mura, D. Morley, S. Sathyavruthan, S. Temelso, R. E. Thomas and L. L. Zhang, *Nat. Methods*, 2013, **10**, 641-+.
15. P. M. Lizardi, X. H. Huang, Z. R. Zhu, P. Bray-Ward, D. C. Thomas and D. C. Ward, *Nat. Genet.*, 1998, **19**, 225-232.
16. B. Schweitzer, S. Roberts, B. Grimwade, W. P. Shao, M. J. Wang, Q. Fu, Q. P. Shu, I. Laroche, Z. M. Zhou, V. T. Tchernev, J. Christiansen, M. Velleca and S. F. Kingsmore, *Nat. Biotechnol.*, 2002, **20**, 359-365.
17. J. Baner, M. Nilsson, M. Mendel-Hartvig and U. Landegren, *Nucleic Acids Res.*, 1998, **26**, 5073-5078.
18. M. Vincent, Y. Xu and H. M. Kong, *Embo Rep.*, 2004, **5**, 795-800.
19. F. Kivlehan, F. Mavre, L. Talini, B. Limoges and D. Marchal, *Analyst*, 2011, **136**, 3635-3642.
20. P. Gill and A. Ghaemi, *Nucleos. Nucleot. Nucl*, 2008, **27**, 224-243.
21. G. M. E. Vandervliet, R. A. F. Schukkink, B. Vangemen, P. Schepers and P. R. Klatser, *J. Gen. Microbiol.*, 1993, **139**, 2423-2429.
22. G.-B. Lee, S.-H. Chen, G.-R. Huang, W.-C. Sung and Y.-H. Lin, *Sensor Actuat. B-Chem.*, 2001, **75**, 142-148.
23. T. Notomi, H. Okayama, H. Masubuchi, T. Yonekawa, K. Watanabe, N. Amino and T. Hase, *Nucleic Acids Res.*, 2000, **28**.
24. Y. Mori, K. Nagamine, N. Tomita and T. Notomi, *Biochem. Bioph. Res. Co.*, 2001, **289**, 150-154.

25. Y. T. Zhou, Q. Huang, J. M. Gao, J. X. Lu, X. Z. Shen and C. H. Fan, *Nucleic Acids Res.*, 2010, **38**.
26. H. Xu, C. Xue, R. B. Zhang, Y. R. Chen, F. Li, Z. F. Shen, L. Jia and Z. S. Wu, *Sensor Actuat. B-Chem.*, 2017, **243**, 1240-1247.
27. H. Y. Liu, L. Li, L. L. Duan, X. Wang, Y. X. Xie, L. L. Tong, Q. Wang and B. Tang, *Anal. Chem.*, 2013, **85**, 7941-7947.
28. H. X. Jiang, Y. P. Xu, L. H. Dai, X. W. Liu and D. M. Kong, *Sensor Actuat. B-Chem.*, 2018, **260**, 70-77.
29. T. Murakami, J. Sumaoka and M. Komiyama, *Nucleic Acids Res.*, 2009, **37**.
30. T. Murakami, J. Sumaoka and M. Komiyama, *Nucleic Acids Res.*, 2012, **40**.
31. B. Yao, Y. C. Liu, M. Y. Tabata, H. T. Zhu and Y. J. Miyahara, *Chem. Commun.*, 2014, **50**, 9704-9706.
32. M. Tabata, Y. Katayama, F. Mannan, A. Seichi, K. Suzuki, T. Goda, A. Matsumoto, Y. Miyahara, *Procedia Eng.*, 2016, **168**, 419-422.
33. A. Seichi, N. Kozuka, Y. Kashima, M. Tabata, T. Goda, A. Matsumoto, N. Iwasawa, D. Citterio, Y. Miyahara and K. Suzuki, *Anal. Sci.*, 2016, **32**, 505-510.
34. C. X. Hu, S. Kalsi, I. Zeimpekis, K. Sun, P. Ashburn, C. Turner, J. M. Sutton and H. Morgan, *Biosens. Bioelectron.*, 2017, **96**, 281-287.
35. D. Han, R. Chand and Y. S. Kim, *Biosens. Bioelectron.*, 2017, **93**, 220-225.
36. R. Lorenzo-Gomez, N. Fernandez-Alonso, R. Miranda-Castro, N. de-los-Santos-Alvarez and M. J. Lobo-Castanon, *Talanta*, 2019, **197**, 406-412.
37. A. Gao, N. Zou, P. Dai, N. Lu, T. Li, Y. Wang, J. Zhao and H. Mao, *Nano Lett.*, 2013, **13**, 4123-4130.
38. B. Veigas, J. Pinto, R. Vinhas, T. Calmeiro, R. Martins, E. Fortunato and P. V. Baptista, *Biosens. Bioelectron.*, 2017, **91**, 788-795.
39. C. Duarte-Guevara, V. V. Swaminathan, B. Reddy, J. C. Huang, Y. S. Liu and R. Bashir, *Rsc Adv.*, 2016, **6**, 103872-103887.
40. R. Polsky, R. Gill, L. Kaganovsky and I. Willner, *Anal. Chem.*, 2006, **78**, 2268-2271.
41. S. Kwakye, V. N. Goral and A. J. Baeumner, *Biosens. Bioelectron.*, 2006, **21**, 2217-2223.
42. M. Steichen, Y. Decrem, E. Godfroid and C. Buess-Herman, *Biosens. Bioelectron.* 2007, **22**, 2237-2243.
43. M. Sanjoh, D. Iizuka, A. Matsumoto and Y. Miyahara, *Org. Lett.*, 2015, **17**, 588-591.
44. T. Goda, K. Masuno, J. Nishida, N. Kosaka, T. Ochiya, A. Matsumoto and Y. Miyahara, *Chem. Commun.*, 2012, **48**, 11942-11944.
45. C. D. Bain, H. A. Biebuyck and G. M. Whitesides, *Langmuir*, 1989, **5**, 723-727.
46. H. Sellers, A. Ulman, Y. Shnidman and J. E. Eilers, *J. Am. Chem. Soc.*, 1993, **115**, 9389-9401.
47. A. de la Escosura-Muniz, L. Baptista-Pires, L. Serrano, L. Altet, O. Francino, A. Sanchez and A. Merkoci, *Small*, 2016, **12**, 205-213.
48. S. Moura-Melo, R. Miranda-Castro, N. de-los-Santos-Alvarez, A. J. Miranda-Ordieres, J. R. D. Santos, R. A. D. Fonseca and M. J. Lobo-Castanon, *Anal. Chem.*, 2015, **87**, 8547-8554.
49. K. Hashimoto, M. Inada and K. Ito, *Anal. Chem.*, 2019, **91**, 3227-3232.
50. Q. Q. Tian, Y. Wang, R. J. Deng, L. Lin, Y. Liu and J. H. Li, *Nanoscale*, 2015, **7**, 987-993.
51. C. Y. Yang, K. Shi, B. T. Dou, Y. Xiang, Y. Q. Chai and R. Yuan, *Acs Appl. Mater. Interfaces*, 2015, **7**, 1188-1193.
52. T. Sakata and Y. Miyahara, *Angew. Chem. Int. Edit.*, 2006, **45**, 2225-2228.
53. J. Zhang, L. L. Wang, M. F. Hou, Y. K. Xia, W. H. He, A. Yan, Y. P. Weng, L. P. Zeng and J. H. Chen, *Biosens. Bioelectron.*, 2018, **102**, 33-40.
54. J. Guo, C. J. Yuan, Q. Yan, Q. Y. Duan, X. L. Li and G. Yi, *Biosens. Bioelectron.*, 2018, **105**, 103-108.
55. Y. H. Yuan, Y. D. Wu, B. Z. Chi, S. H. Wen, R. P. Lian and J. D. Qiu, *Biosens. Bioelectron.*, 2017, **97**, 325-331.
56. H. L. Shuai, K. J. Huang, Y. X. Chen, L. X. Fang and M. P. Jia, *Biosens. Bioelectron.*, 2017, **89**, 989-997.
57. W. Ma, B. Situ, W. F. Lv, B. Li, X. M. Yin, P. Vadgama, L. Zheng and W. Wang, *Biosens. Bioelectron.*, 2016, **80**, 344-351.
58. B. C. Li, F. Liu, Y. Y. Peng, Y. L. Zhou, W. X. Fan, H. S. Yin, S. Y. Ai and X. S. Zhang, *Biosens. Bioelectron.*, 2016, **79**, 307-312.
59. R. M. Torrente-Rodriguez, S. Campuzano, V. R. V. Montiel, J. J. Montoya and J. M. Pingarron, *Biosens. Bioelectron.*, 2016, **86**, 516-521.
60. X. Y. Li, G. Peng, F. Cui, Q. Y. Qiu, X. J. Chen and H. Huang, *Biosens. Bioelectron.*, 2018, **113**, 116-123.
61. W. Lu, Q. P. Yuan, Z. L. Yang and B. Yao, *Biosens. Bioelectron.*, 2017, **90**, 258-263.
62. M. H. Lu, L. F. Xu, X. N. Zhang, R. Xiao and Y. M. Wang, *Biosens. Bioelectron.*, 2015, **73**, 195-201.
63. C. Y. Yu, G. Y. Ang, K. G. Chan, K. K. B. Singh and Y. Y. Chan, *Biosens. Bioelectron.*, 2015, **70**, 282-288.
64. J. Luo, X. E. Fang, D. X. Ye, H. X. Li, H. Chen, S. Zhang and J. L. Kong, *Biosens. Bioelectron.*, 2014, **60**, 84-91.
65. G. Sozzi, D. Conte, M. E. Leon, R. Cirincione, L. Roz, C. Ratcliffe, E. Roz, N. Cirenei, M. Bellomi, G. Pelosi, M. A. Pierotti and U. Pastorino, *J. Clin. Oncol.*, 2003, **21**, 3902-3908.
66. K. Kim, D. G. Shin, M. K. Park, S. H. Baik, T. H. Kim, S. Kim and S. Lee, *Ann. Surg. Treat. Res.*, 2014, **86**, 136-142.
67. X. Q. Chen, H. Bonnefoi, S. Diebold-Berger, J. Lyautey, C. Lederrey, E. Faltin-Traub, M. Stroun and P. Anker, *Clin. Cancer Res.*, 1999, **5**, 2297-2303.
68. G. Sozzi, D. Conte, L. Mariani, S. Lo Vullo, L. Roz, C. Lombardo, M. A. Pierotti and L. Tavecchio, *Cancer Res.*, 2001, **61**, 4675-4678.
69. C. Bettegowda, M. Sausen, R. J. Leary, I. Kinde, Y. X. Wang, N. Agrawal, B. R. Bartlett, H. Wang, B. Luber, R. M. Alani, E. S. Antonarakis, N. S. Azad, A. Bardelli, H. Brem, J. L. Cameron, C. C. Lee, L. A. Fecher, G. L. Gallia, P. Gibbs, D. Le, R. L. Giuntoli, M. Goggins, M. D. Hogarty, M. Holdhoff, S. M. Hong, Y. C. Jiao, H. H. Juhl, J. J. Kim, G. Siravegna, D. A. Laheru, C. Lauricella, M. Lim, E. J. Lipson, S. K. N. Marie, G. J. Netto, K. S. Oliner, A. Olivi, L. Olsson, G. J. Riggins, A. Sartore-Bianchi, K. Schmidt, I. M. Shih, S. M. Oba-Shinjo, S. Siena, D. Theodorescu, J. N. Tie, T. T. Harkins, S. Veronese, T. L. Wang, J. D. Weingart, C. L. Wolfgang, L. D. Wood, D. M. Xing, R. H. Hruban, J. Wu, P. J. Allen, C. M. Schmidt, M. A. Choti, V. E. Velculescu, K. W. Kinzler, B. Vogelstein, N. Papadopoulos and A. J. Luis, *Sci. Transl. Med.*, 2014, **6**.
70. A. R. Thierry, F. Mouliere, S. El Messaoudi, C. Mollevi, E. Lopez-Crapez, F. Rolet, B. Gillet, C. Gongora, P. Dechelotte,

B. Robert, M. Del Rio, P. J. Lamy, F. Bibeau, M. Nouaille, V. Loriot, A. S. Jarrousse, F. Molina, M. Mathonnet, D. Pezet and M. Ychou, *Nat. Med.*, 2014, **20**, 430-+.

71. E. Heitzer, M. Auer, P. Ulz, J. B. Geigl and M. R. Speicher, *Genome Med.*, 2013, **5**.
72. K. C. A. Chan, P. Y. Jiang, C. W. M. Chan, K. Sun, J. Wong, E. P. Hui, S. L. Chan, W. C. Chan, D. S. C. Hui, S. S. M. Ng, H. L. Y. Chan, C. S. C. Wong, B. B. Y. Ma, A. T. C. Chan, P. B. S. Lai, H. Sun, R. W. K. Chiu and Y. M. D. Lo, *P. Natl. Acad. Sci. USA*, 2013, **110**, 18761-18768.
73. K. C. A. Chan, P. Y. Jiang, Y. W. L. Zheng, G. J. W. Liao, H. Sun, J. Wong, S. S. N. Siu, W. C. Chan, S. L. Chan, A. T. C. Chan, P. B. S. Lai, R. W. K. Chiu and Y. M. D. Lo, *Clin. Chem.*, 2013, **59**, 211-224.
74. G. Siravegna, S. Marsoni, S. Siena and A. Bardelli, *Nat. Rev. Clin. Oncol.*, 2017, **14**, 531-548.

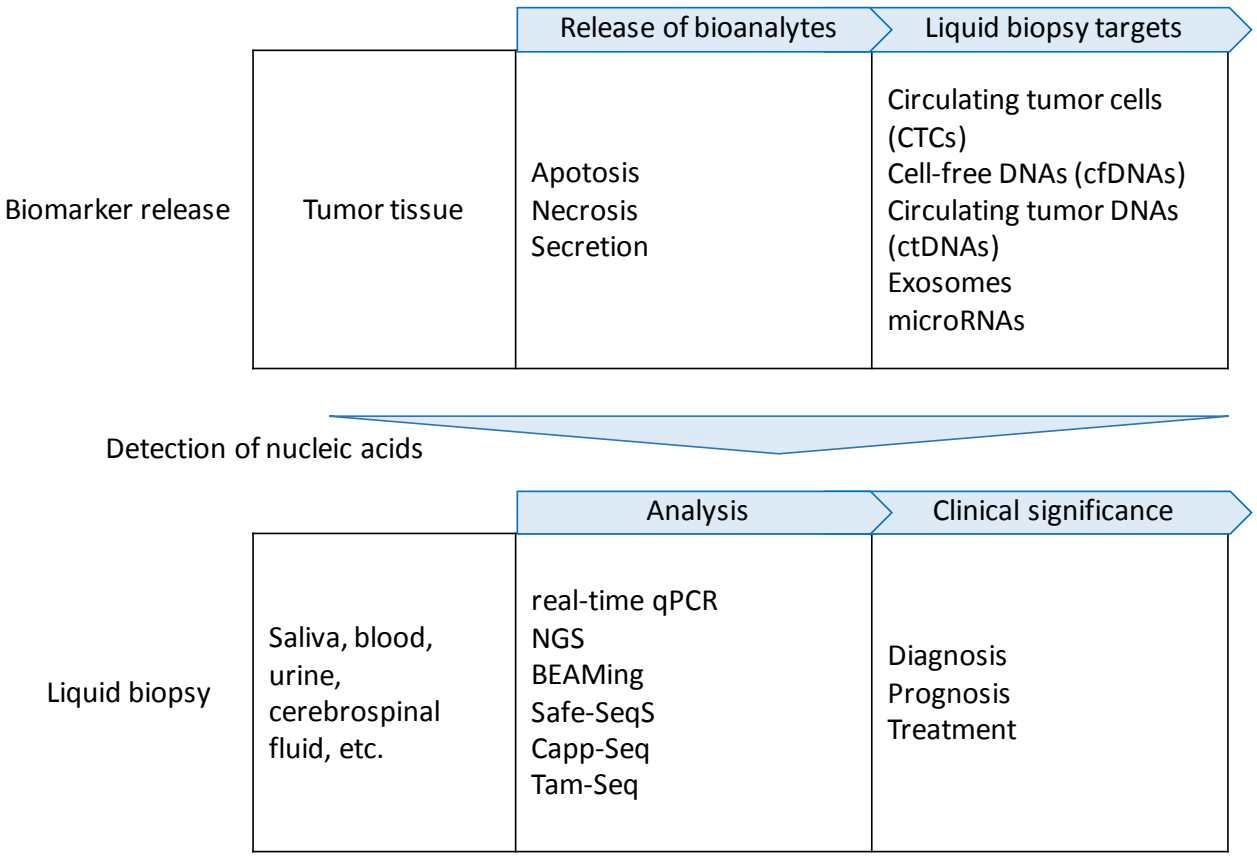

Fig. 1

Schematic illustration of the workflow in liquid biopsy targeting on nucleic acids. In the analysis part, optical detection methods are mainly used as represented by real-time qPCR, however, there is room for replacing electrical devices combined with isothermal nucleic acid amplification methods.

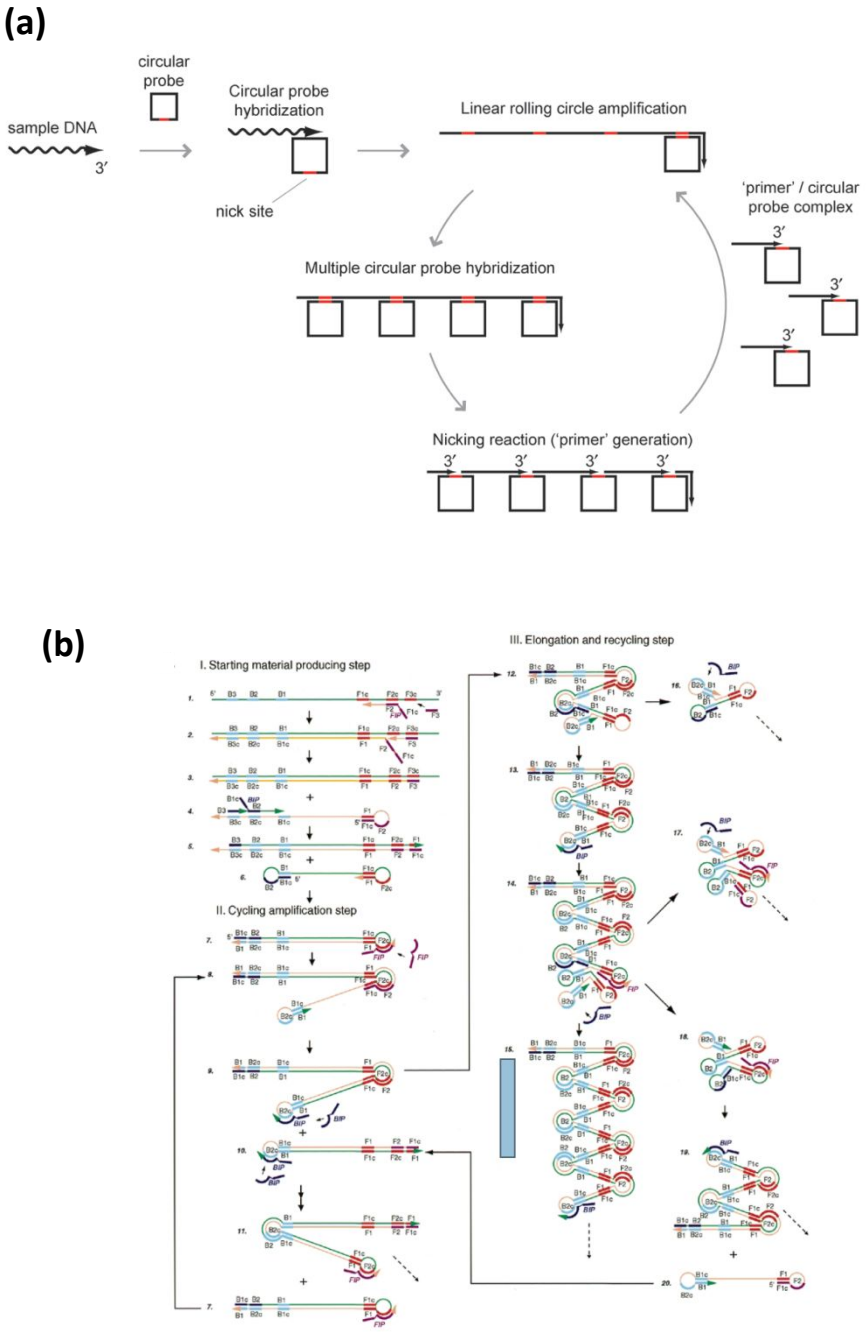

Fig. 2

Schematic illustrations of exponential isothermal amplification methods. (a) PG-RCA. (b) LAMP. Fig. 1(a) is reprinted from ref. 30 by permission from Oxford University Press, and Fig. 1(b) is reprinted by permission from Oxford University Press from ref. 23.

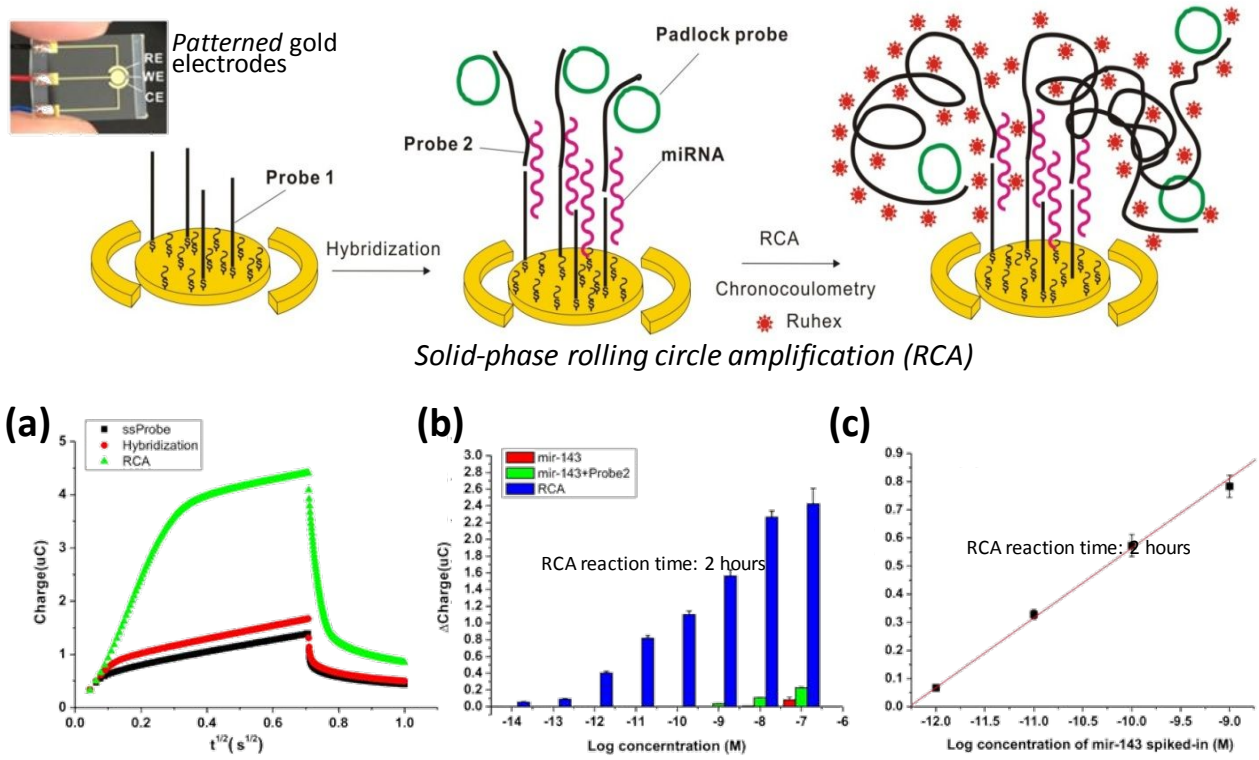

Fig. 3

Solid-phase rolling circle amplification and chronocoulometry (RCA-CC) for microRNA detection. (a) Chronocoulometry plots of immobilization of a single-stranded DNA probe on gold electrodes, the same probe after hybridization with 10 nM of target molecules, and the same probe after four-hour RCA amplification. (b) Sensitivity of RCA-CC assay for detection of mir-143. Detection limit was 100 fM, and detection range was from 100 fM to 1 nM. (c) Detection of mir-143 spiked in human blood samples. Detection limit of mir-143 in blood samples was 1 pM. Dynamic range was from 1 pM to 1 nM. Reprinted by permission from Royal Society of Chemistry: ref. 34, copyright 2014.

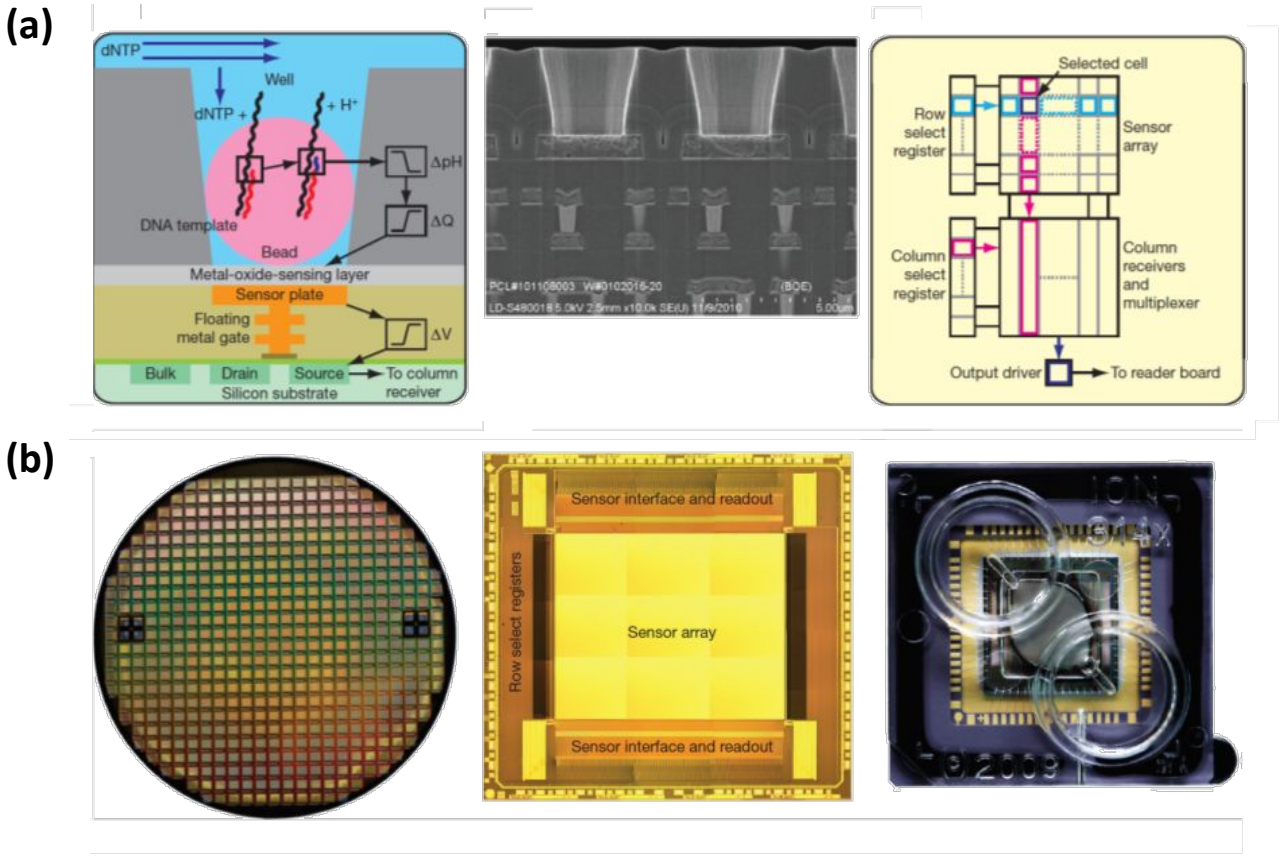

Fig. 4

Commercialized ISFET-based DNA sequencer. (a) Schematic illustration of sequencing mechanism and electron micrograph showing wells. (b) Ion chip on wafer, die, and chip packaging. Reprinted by permission from Springer Nature: ref. 13, copyright 2011.

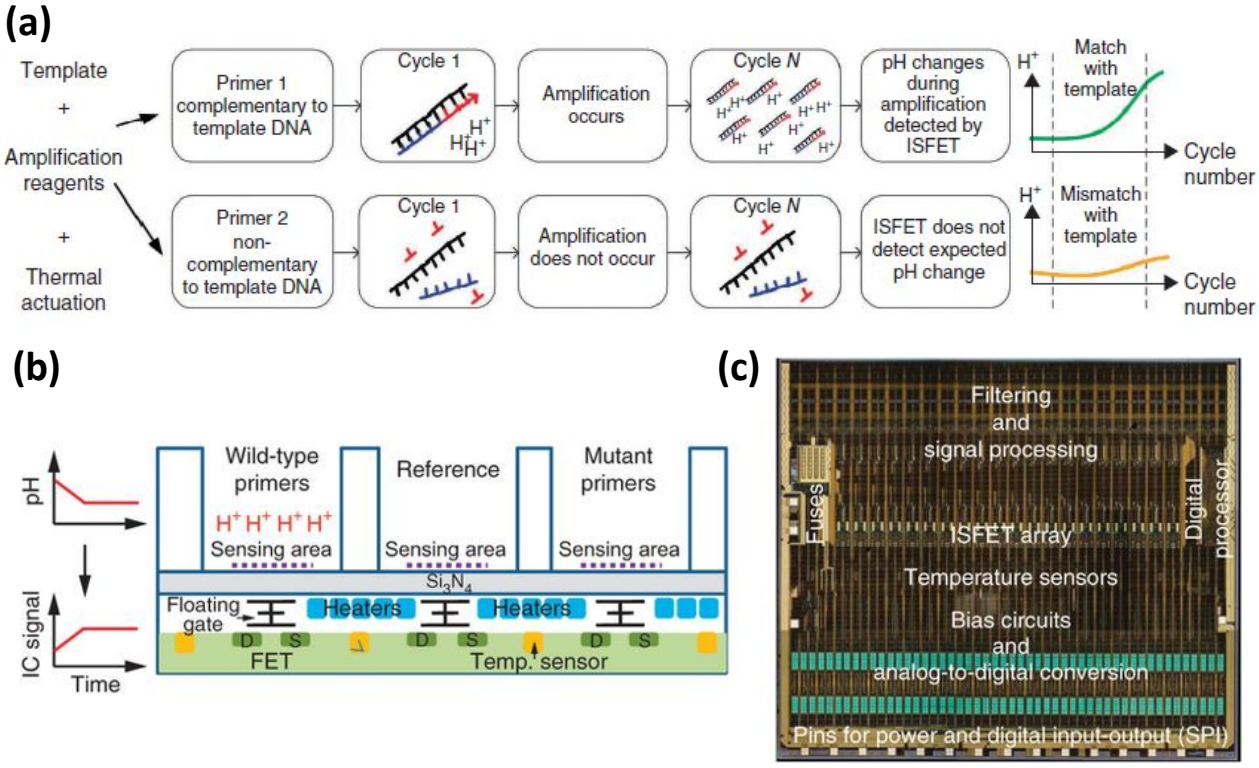

Fig. 5

pH-sensing integrated circuit. (a) pH-based amplification detection strategy. The amplification process of PCR or LAMP was performed under low buffering capacity conditions in order to quantitatively detect pH change with the ISFET. (b) A simplified cross-section of the ISFET array area (floating gate, source (S) and drain (D)), temperature sensors (yellow squares), and digitally controlled resistive heater elements (blue squares) (c) CMOS-fabricated chip (right) showing key architectural modules. Reprinted by permission from Springer Nature Publishing AG: ref. 14, copyright 2013.

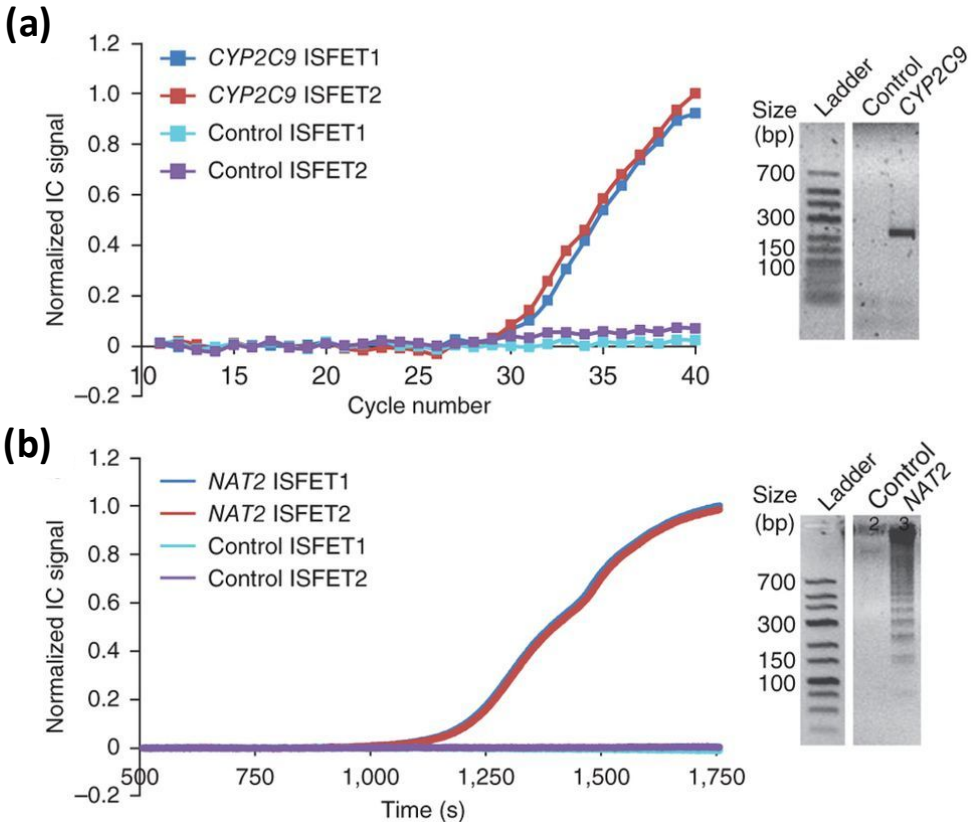

Fig. 6

On-chip amplification and detection using pH-PCR and pH-LAMP (a) Representative on-chip pH-PCR amplification curves of homozygous wild-type CYP2C9*1 allele. The control represents the no-template reaction. The amplification curves represent the integrated circuit (IC) signal for the two ISFETs in a reaction chamber. Gels show product recovered from the chip at the end of the reaction (2% agarose gels, visualized by SYBR Green). (b) Representative on-chip pH-LAMP amplification curves of NAT2. The control represents the no-template reaction. The amplification curves represent the IC signal for the two ISFETs in a reaction chamber. Gels show products recovered from the chip at the end of the isothermal reaction, as in (a). Reprinted by permission from Springer Nature Publishing AG: ref. 14, copyright 2013.

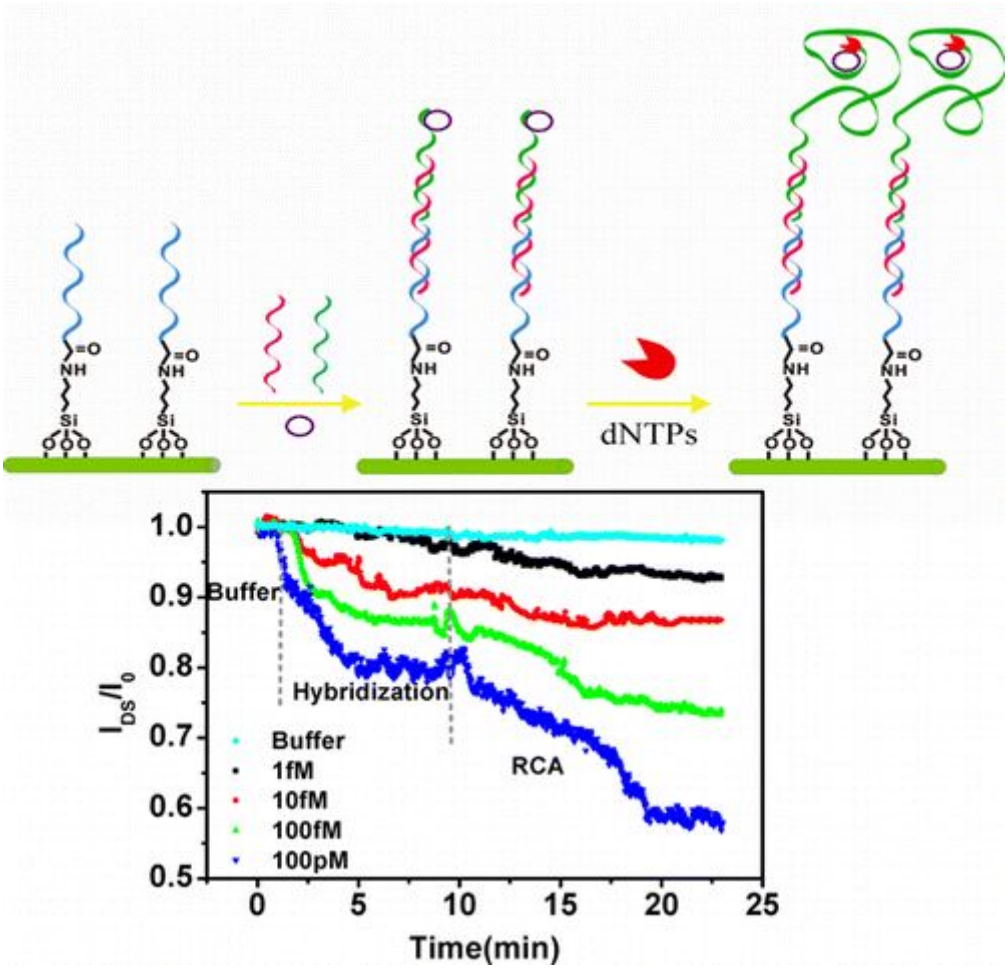

Fig. 7

Rapid, label-free, and specific DNA detection by applying rolling circle amplification (RCA) based on silicon nanowire field-effect transistor (SiNW-FET). Reprinted by permission from American Chemical Society: ref. 44, copyright 2013.

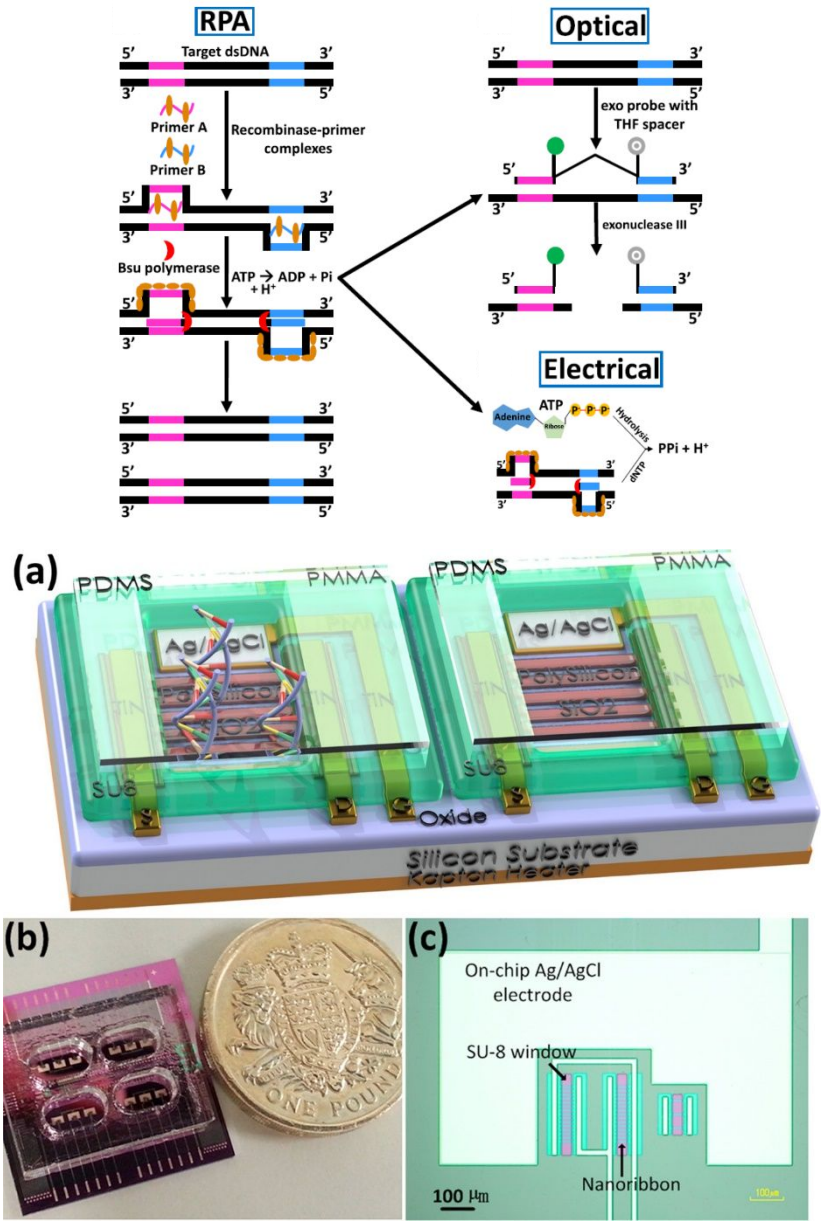

Fig. 8

The recombinase polymerase reaction (RPA) was combined with thin-film transistor nanoribbon (TFT NR). (a) Schematic diagram of the TFT sensor showing the measurement configuration (not to scale). Two NR transistors are used in a differential configuration. Each sensor has an integrated Ag/AgCl reference electrode. Both contain RPA chemistry and primers, but only one has target DNA; (b) Photograph of the device. Each Si chip comprises 12 separate sensors in four PMMA wells that contain the sample. To prevent evaporation, the wells were covered with a thin PDMS lid; (c) Microscope image of a single NR sensor made of 30 nanoribbons connected in parallel, each 40 µm long. Also shown are the metal tracks that connect to the two sets of nanoribbons. The entire Si chip is covered in SU8, except for small windows that expose the sensing area as shown in the figure. The entire region is also surrounded on three sides by a large integrated Ag/AgCl reference electrode. Reprinted by permission from Elsevier B.V.: ref. 45, copyright 2017.

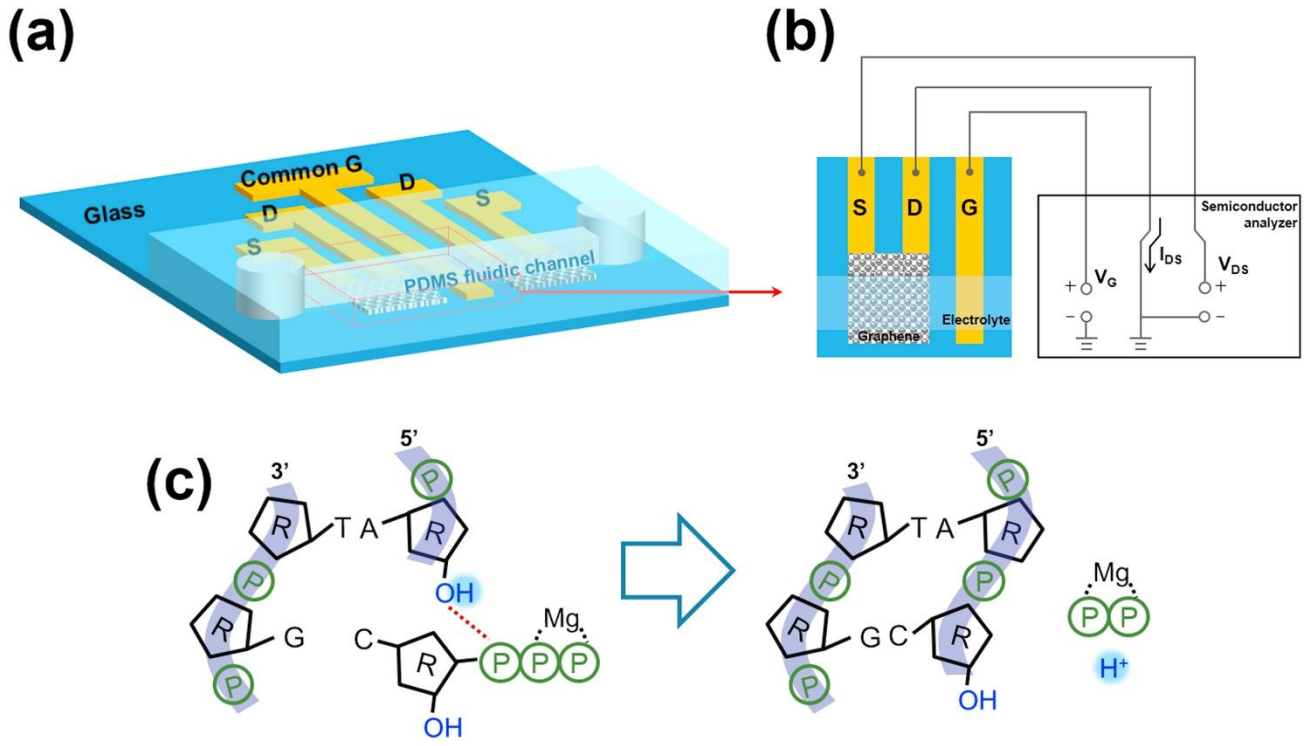

Fig. 9

Solution-gated graphene FET (SG-FET): (a) schematic of SG-FET couple with common gate, where S, D, and G are source, drain, and gate electrodes respectively, (b) measurement setup of a single SG-FET, and (c) mechanism of proton release during DNA synthesis. Reprinted by permission from Elsevier B.V.: ref. 46, copyright 2017.

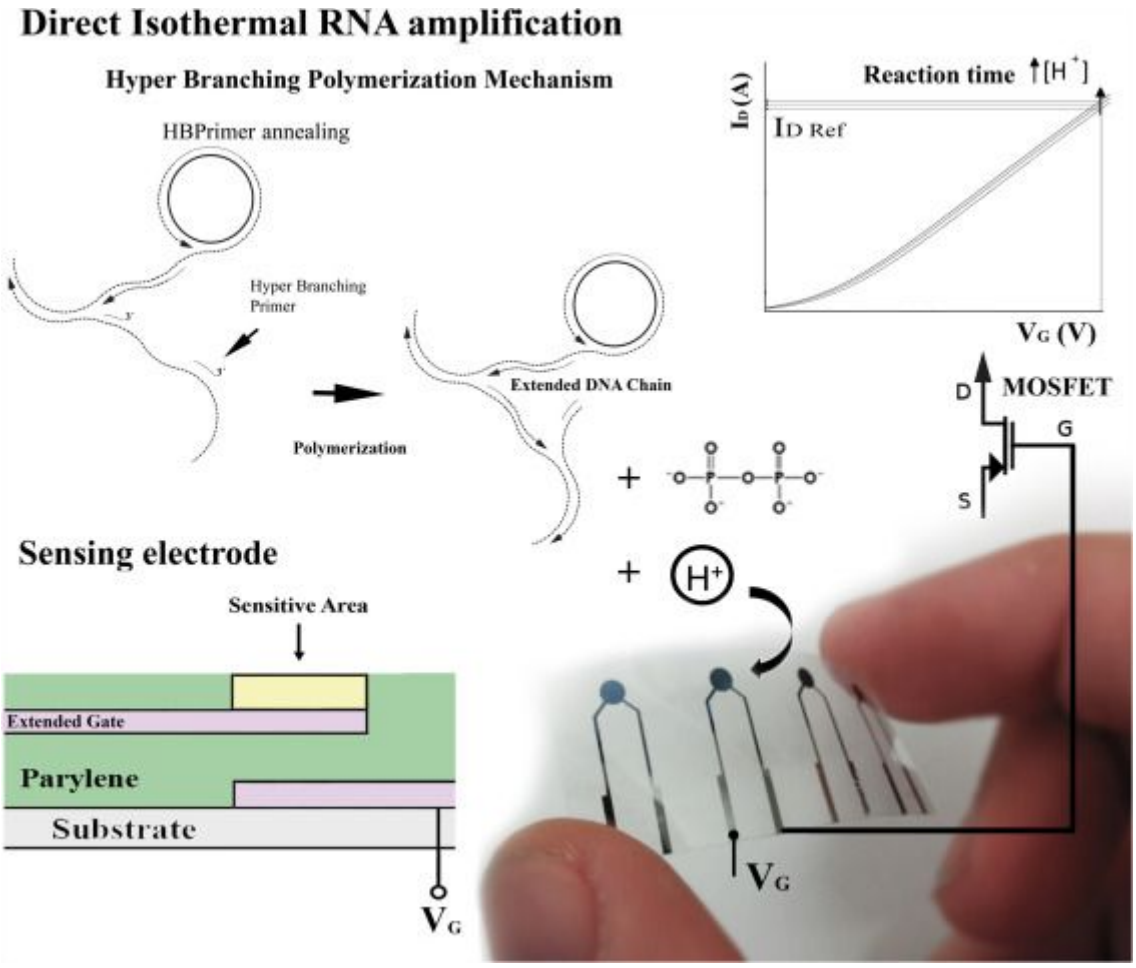

Fig. 10

Charge-modulated extended gate ISFET biosensor. Sensing electrode comprising a stacked control/sensing electrode and a standard commercial transistor. The elongation reaction results in accumulation of protons (lowering the solution pH) proportional to the number of incorporated nucleotides. The RCA amplification scheme relies on a padlock probe activated by a ligase dependent reaction. After DNA/RNA conversion, Φ29 starts a cyclic polymerization by strand displacement activity. Additionally, two primer sequences can be added for a hyperbranched mechanism, leading to exponential reaction kinetics. Reprinted by permission from Elsevier B.V.: ref. 47, copyright 2017.